

High Speed Continuous Variable Source-Independent Quantum Random Number Generation

Bingjie Xu^{1,2}, Zhengyu Li^{3,*}, Jie Yang¹, Shihai Wei¹, Qi Su², Wei Huang¹, Yichen Zhang⁴, and Hong Guo³

*1 Science and Technology on Security Communication Laboratory,
Institute of Southwestern Communication, Chengdu 610041, China*

2 State Key Laboratory of Cryptography, Beijing 100878, China

*3 State Key Laboratory of Advanced Optical Communication Systems and Networks,
School of Electronics Engineering and Computer Science,*

and Center for Quantum Information Technology, Peking University, Beijing 100871, China and

*4 State Key Laboratory of Information Photonics and Optical Communications,
Beijing University of Posts and Telecommunications, Beijing 100876, China*

(Dated: December 14, 2024)

As a fundamental phenomenon in nature, randomness has a wide range of applications in the fields of science and engineering. Among different types of random number generators (RNG), quantum random number generator (QRNG) is a kind of promising RNG as it can provide provable true random numbers based on the inherent randomness of fundamental quantum processes. Nevertheless, the randomness from a QRNG can be diminished (or even destroyed) if the devices (especially the entropy source devices) are not perfect or ill-characterized. To eliminate the practical security loopholes from the source, source-independent QRNGs, which allow the source to have arbitrary and unknown dimensions, have been introduced and become one of the most important semi-device-independent QRNGs. Herein a method that enables ultra-fast unpredictable quantum random number generation from quadrature fluctuations of quantum optical field without any assumptions on the input states is proposed. Particularly, to estimate a lower bound on the extractable randomness that is independent from side information held by an eavesdropper, a new security analysis framework is established based on the extremality of Gaussian states, which can be easily extended to design and analyze new semi-device-independent continuous variable QRNG protocols. Moreover, the practical imperfections of the QRNG including the effects of excess noise, finite sampling range and resolution are taken into account and quantitatively analyzed. Finally, the proposed method is experimentally demonstrated to obtain a high secure random number generation rate of 15.07 Gbits/s.

PACS numbers: 03.67.Dd, 03.67.Hk

I. INTRODUCTION

Random numbers are of extreme importance for a wide range of applications in both scientific and commercial fields [1], such as numerical simulations, lottery games and cryptography. A significant example is the quantum key distribution (QKD), in which the true random numbers are essential for both quantum states preparation and detection to guarantee unconditional security [2–4]. Classical pseudo random number generators (PRNG), which are based on the computational algorithms, have been widely used in modern information systems. However, due to the deterministic and thus predictable features of the algorithms, PRNG are not suitable for certain applications where true randomness is required. Distinct from the PRNG, true random number generators (TRNG) extract randomness from physical random processes [5]. An important type of TRNGs is the quantum random number generator (QRNG), which is based on the intrinsic randomness of fundamental quantum processes and can provide truly unpredictable and irreproducible random numbers [6–8].

The existing QRNG protocols can be mainly classified into three different categories as in Ref. [7], i.e. the practical, device-independent and semi-device-independent QRNGs. Till now, various practical QRNG protocols, which can realize a high random number generation rate with relatively

low cost [7], have been proposed and demonstrated, including measuring photon path [9, 10], photon arrival time [11–15], photon number distribution [16–19], vacuum fluctuation [20–25], phase noise [26–36] and amplified spontaneous emission noise [37–41] of quantum states. However, practical QRNGs can produce true random numbers with information-theoretical provable security only if the randomness source and detection devices are trusted and fulfill with the model assumptions, which usually fails in cases that the devices are complex or controlled by eavesdroppers [7]. To avoid the defects, device-independent (DI) QRNG, which can generate verifiable randomness without assumptions on the source and measurement devices by observing the violation of Bell's inequality, have been proposed [42, 43]. Although DI-QRNG protocols (including both randomness expansion [44–47] and amplification [48, 49] protocols) have advantage of the self-testing randomness, they are highly challenging in realistic implementations (e.g. not loss tolerant), and the generation speed is usually too slow for practical applications [47]. Thus, QRNG protocol with reasonable assumptions and high practical performance is meaningful and greatly needed. To balance the performance and the security, the semi-device-independent QRNG provides a trade-off between the practical and device independent QRNGs, where high speed and low-cost informational provable randomness can be generated under several reasonable assumptions without requiring trusted and complete model assumptions on all devices [7, 50–54]. Particularly, as the quantum entropy source device is usually

* lizhengyu@pku.edu.cn

a complicated physical system in practice and crucial for randomness generation, any deviations in the real-life implementation from its model assumptions may affect the output randomness [50]. Therefore, how to design a QRNG protocol without any assumption on the source device become an important and meaningful issue. To solve this problem, source-independent (SI) QRNG protocols based on measuring single photon path [50] and vacuum fluctuation [51] are proposed and experimentally verified, in which the output randomness can be certified even when the source is uncharacterized and untrusted, and the corresponding random number generation rates are 5 Kbits/s and 1.7 Gbits/s, respectively.

In this paper, a source-independent continuous-variable (CV) QRNG protocol, which requires no assumption on the source, is proposed by measuring quadrature fluctuations of quantum optical field and experimentally demonstrated. Compared to previous works where security analysis is based on entropic uncertainty [51], we demonstrate a new method to estimate a lower bound on the extractable randomness independent from classical or quantum side information held by an eavesdropper (Eve) based on the extremality of Gaussian states [55]. The security analysis model shows similarity to that of CV-QKD [56], where rich theoretical tools exist, and can be easily extended to design and analyze new semi-device-independent CV-QRNG protocols, e.g. semi-device-independent CV-QRNG protocols with different input states or measurements. Furthermore, several practical issues of the protocol, including excess noise, finite detection range and resolution are quantitatively analyzed, and the optimal choices of experimental parameters are discussed. It is shown that the proposed protocol is significantly resistant to noise and loss, which can be realized with off-the-shelf commercial devices and enable ultra-fast randomness generation rates. The final experimental secure random number generation rate, which reaches up to 15 Gbits/s based on the proposed method, is much faster than previous SI-QRNG results.

II. SI-CV-QRNG PROTOCOL

A schematic of the proposed SI-CV-QRNG protocol is described as follows (as shown in Fig. 1):

(i) Randomness Source Preparation: Eve prepares an untrusted and uncharacterized source with quantum states ρ_A in arbitrary dimension, where Eve has access to a quantum system E correlated with system A , and sends ρ_A to the balanced homodyne measurement device of Alice.

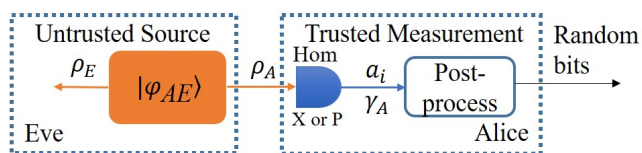


FIG. 1. (color online) Schematic of the proposed SI-CV-QRNG protocol.

(ii) Measurement: Alice measures the X quadrature of ρ_A to generate random bits with measurement results a_i , and randomly samples n_c (check samples) out of n_{tot} (total measurements) to measure P quadrature of ρ_A to check the purity of the input states based on a random initial seed with length t . The measurement is assumed to be trusted and well calibrated, and all the excess noise is assumed to be introduced by a quantum correlated Eve as in Refs. [51, 56].

(iii) Parameter Estimation: The covariance matrix (CM) γ_A of ρ_A is estimated based on Alice's measurement results on quadratures X and P ,

$$\gamma_A = \begin{bmatrix} V_x & c \\ c & V_p \end{bmatrix}, \quad (1)$$

where V_x and V_p are the variance of X and P quadratures, and c is the co-variance between X and P quadratures for ρ_A .

(iv) Randomness Estimation and Extraction: Alice can extract asymptotically $(n_{tot} - n_c)(H(a_i) - S(a_i : E)) - t$ final randomness in n_{tot} measurements by using informational provable randomness extractor, such as Toeplitz-matrix hashing extractor, where $H(a_i)$ is the Shannon entropy of Alice's measurement results a_i and $S(a_i : E)$ is the quantum mutual information between Eve's quantum state ρ_E and Alice's measurement results a_i .

In this protocol, no assumptions are made on the dimensions and purity of the input states [51], which are difficult to verify experimentally. Indeed, it is typically difficult to prepare and keep a real quantum system in a pure state. The detection is assumed to be trusted and all the excess noise is due to a quantum correlated Eve, which shows similarity with security analysis of CV-QKD and is the most conservative option [56]. In fact, the method can also take into account the classical side information hold by Eve effectively as in Refs. [23, 51].

III. SECURITY ANALYSIS

Suppose Alice's homodyne detection is ideal (with infinite range and resolution), then the measurement results of quadrature X for ρ_A is a continuous variable a . The asymptotically extractable randomness per measurement that uniform and uncorrelated from quantum side information held by Eve is,

$$R(a|E) = H(a) - S(a : E), \quad (2)$$

where $H(a)$ is the classical Shannon entropy of Alice's ideal measurement results on X , which is not well-defined for continuous variable (Alice actually gets a discrete variable a_i in practice as explained below), and $S(a : E)$ is the Holevo's bound between Eve's quantum state ρ_E and Alice's measurement results a , which is an upper bound of Eve's quantum side information. We assume Eve holds a purification of the input state $\rho_A = \text{Tr}_E\{|\varphi_{AE}\rangle\langle\varphi_{AE}|\}$, which is optimal for Eve. Then one has,

$$S(a : E) = S(\rho_E) - \int p(a) S(\rho_{E|a}) da = S(\rho_A), \quad (3)$$

where $p(a)$ is the probability density distribution of Alice's measurement results, and $\rho_{E|a}$ is the quantum state held by Eve given that Alice's measurement result is a . If the CM of ρ_A is known, one can prove that the von Neumann entropy of an arbitrary ρ_A is upper bounded by that of a Gaussian state ρ_A^G with the same CM based on the extremality of Gaussian states [55], which means $S(\rho_A) \leq S(\rho_A^G)$. Then, one has

$$R(a|E) = H(a) - S(\rho_A) \geq H(a) - S(\rho_A^G). \quad (4)$$

Alternatively, one can verify that R fits all the three conditions for Lemma 1 in Ref. [55], which also infers that $R(\rho_A) \geq R(\rho_A^G) = H(a) - S(\rho_A^G)$ given a finite CM of ρ_A . In fact, the security of CV-QKD protocols against collective attacks have been proved with similar methods [56].

In practice, Alice's coarse-grained homodyne measurement is imperfect (with finite range and resolution) and modeled as follows. First, Alice utilizes an ideal homodyne detector to measure the quadrature of input states with continuous output a following probability density distribution $p(a)$, which cannot be read. Second, Alice digitizes the continuous data a into n bits a_i following probability distribution $p_{dis}(a_i)$ by an ADC with sampling range $[-N + \Delta/2, N - \Delta/2]$ and resolution n (see Appendix A for details) [23], which is the actual output of a real-life homodyne detector. Upon measurement, the continuous signal a is discretized into a_i over 2^n bins with precision $\Delta = N/2^{n-1}$. Then, the extractable randomness is reduced to

$$R_{dis}(a_i|E) = H(a_i) - S(a_i : E), \quad (5)$$

where $H(a_i)$ is the Shannon entropy of discrete variable a_i , which is well-defined, and $S(a_i : E)$ is the Holevo's bound between Eve's quantum state ρ_E and Alice's measurement results a_i . $H(a_i)$ can be calculated easily based on Alice's measurement results a_i , while there are no direct way to compute $S(a_i : E)$.

To get a lower bound for the extractable randomness, one needs to upper bound $S(a_i : E)$. Fortunately, one can prove that

$$S(a_i : E) \leq S(a : E), \quad (6)$$

which indicates that local operation on one part of a state cannot increase the mutual information between two parties (see Appendix B for detail proofs). Furthermore, $S(a : E) = S(\rho_A) \leq S(\rho_A^G)$, then one has

$$R_{dis}(a_i|E) \geq H(a_i) - S(a : E) \geq H(a_i) - S(\rho_A^G). \quad (7)$$

The remaining question is how to upper bound $S(\rho_A^G)$ given Alice's digitized measurement results a_i . Due to the digitization process, we lose the information about the distribution of a inside the discrete bins and outside the sampling range, thus one cannot calculate the exact CM for ρ_A based on a_i . However, given each a_i corresponding to each continuous a with known upper and lower bound, one can estimate an upper bound \bar{V}_x (\bar{V}_p) for the variance of X (P) quadrature for ρ_A

with a simple strategy (see Appendix C for details). Then,

$$S(a_i : E) \leq S(\rho_A^G) \leq \frac{\bar{\lambda} + 1}{2} \log_2 \frac{\bar{\lambda} + 1}{2} - \frac{\bar{\lambda} - 1}{2} \log_2 \frac{\bar{\lambda} - 1}{2}, \quad (8)$$

where $\bar{\lambda} = \sqrt{\bar{V}_x \bar{V}_p}$, and we set $c = 0$ to get the upper bound of $\bar{\lambda}$.

In our protocol, the input state is expected (by Alice) to be a vacuum state if not disturbed by Eve, while in fact it could be an arbitrary quantum state ρ_A prepared by Eve (e. g. thermal state or squeezed state). Define the variance of vacuum fluctuation as $\sigma_{vac}^2 = 1$ (all the relevant quantities are normalized by vacuum fluctuation in the following). In practice, the measurement results of quantum state are unavoidable mixed with excess noise ε (due to classical or quantum side information held by Eve), which is the difference between measured quadrature variance (σ^2) and the expected vacuum fluctuation, i.e. $\varepsilon = \sigma^2 - 1$. Define the QCNR (quantum to classical noise ratio) as $10 \log_{10}(1/\varepsilon)$. A typical example is that $\sigma^2 = V_x = V_p = 1 + \varepsilon$, due to a classical Eve that controls symmetric electronic noise of the detection [23] or a quantum Eve that holds a purification of input state [51]. In this case, Alice's homodyne measurement results a on quadrature X (or P) is expected to be a continuous variable following Gaussian distribution with variance σ^2 and null mean value,

$$p(a) = \frac{1}{\sqrt{2\pi}\sigma} \exp\left(-\frac{a^2}{2\sigma^2}\right). \quad (9)$$

The corresponding CM of ρ_A is $\gamma_A = \begin{bmatrix} 1 + \varepsilon & 0 \\ 0 & 1 + \varepsilon \end{bmatrix}$, with upper bounded

$$S(a : E) \leq S(\rho_A^G) = \left(\frac{\varepsilon}{2} + 1\right) \log\left(\frac{\varepsilon}{2} + 1\right) - \frac{\varepsilon}{2} \log \frac{\varepsilon}{2}. \quad (10)$$

Then, the corresponding probability distribution $p_{dis}(a_i)$ after discrete sampling is

$$p_{dis}(a_i) = \begin{cases} \frac{1}{2} \operatorname{erfc}\left(\frac{N-0.5\Delta}{\sqrt{2}\sigma}\right), & i = i_{\min} \\ \frac{1}{2} \operatorname{erf}\left(\frac{i+0.5}{\sqrt{2}\sigma}\Delta\right) - \frac{1}{2} \operatorname{erf}\left(\frac{i-0.5}{\sqrt{2}\sigma}\Delta\right), & i_{\min} < i < i_{\max} \\ \frac{1}{2} \operatorname{erfc}\left(\frac{N-1.5\Delta}{\sqrt{2}\sigma}\right), & i = i_{\max} \end{cases} \quad (11)$$

with $i_{\min} = -2^{n-1}$ and $i_{\max} = 2^{n-1} - 1$. Then one can estimate the upper bounds of V_x , V_p and $S(a_i : E)$ as in Appendix C. Note that the model in Eqs. (4) and (5) also fit with the asymmetric quantum states (i.e. $V_x \neq V_p$).

In the above security analysis model, no assumptions are made on the input states, which remove Eve's side-information on source. Therefore, the extracted randomness is source device loophole-free.

IV. PRACTICAL ISSUES AND NUMERICAL SIMULATIONS

The practical issues of the proposed QRNG protocol, such as sampling range N , precision n of homodyne detection, and

excess noise ε will directly affect the performance of the protocol. Roughly speaking, the performance of the protocol attains near optimal by setting $N \in [3\sigma, 5\sigma]$ given fixed n and ε , increases (decreases) with n (ε) given fixed N , and shows resistant to excess noise.

A. Effects of finite sampling range

The finite sampling range will make us lose the information about probability distribution of a outside the detection range, directly influence the measured probability distribution $p_{dis}(a_i)$ given $p(a)$ (as in Appendix A), and thus affect the classical information $H(a_i)$ of measurement results (as in Fig. 2(a)), the estimated upper bound \bar{V}_x (as in Appendix C) and Eve's information $S(a_i : E)$ (as in Fig. 2(b)). For a fixed resolution n , the effects of dynamical sampling range N are:

1. If it is too small, the measurement outcomes become more predictable, and the Shannon entropy will reduce dramatically as in Fig. 2(a) due to the oversaturated measurement results, which will compromise both the rate and the security of the random number generation. Meanwhile, one cannot estimate precisely the CM of the input states ρ_A , i.e. overestimate the variance of a based on a_i , thus overestimate Eve's information $S(a_i : E)$ (as in Fig. 2(b)).
2. If it is chosen too large, most sampling bins will be unoccupied, and most measurement results lie in central bins, which will reduce the extractable randomness.

Finally, the extractable randomness $R_{dis}(a_i|E)$ increases significantly with N when it is small, and reduces slowly after the optimal choice of N as in 2(c). In practice, the absolute

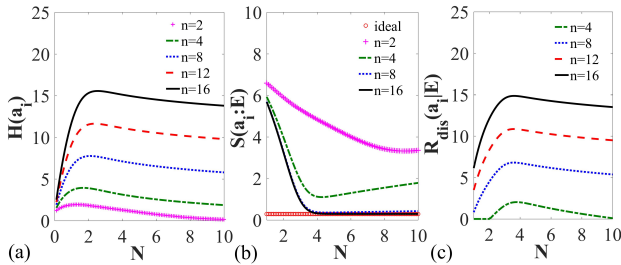


FIG. 2. (color online) Simulation results for (a) Shannon entropy $H(a_i)$ of Alice's measurement results, (b) upper bound of Eve's information $S(a_i : E)$ and (c) extractable quantum randomness $R_{dis}(a_i|E)$ as a function of sampling range N with resolution $n = 2, 4, 8, 12$ and 16 , respectively. The probability distribution of a_i is simulated by Eq. (11) and $H(a_i) = -\sum_{i=i_{min}}^{i=i_{max}} p_{dis}(a_i) \log_2(p_{dis}(a_i))$, based on which the upper bound of quadratures variance \bar{V}_x (\bar{V}_p) for ρ_A is estimated. Then one has $S(a_i : E) \leq \frac{\bar{\lambda}+1}{2} \log_2 \frac{\bar{\lambda}+1}{2} - \frac{\bar{\lambda}-1}{2} \log_2 \frac{\bar{\lambda}-1}{2}$, $\bar{\lambda} = \sqrt{\bar{V}_x \bar{V}_p}$. The ideal case in (b) corresponds to the estimated upper bound of $S(a_i : E)$ when $N \rightarrow \infty, n \rightarrow \infty$ as in Eq. (10). Finally, $R_{dis}(a_i|E)$ is estimated by Eqs. (8) and (9). The excess noise is chosen to be $\varepsilon = 0.1$ and ρ_A is assumed to be a symmetric Gaussian state with $V_x = V_p = 1 + \varepsilon$.

value of N for an ADC device is usually fixed. However, one can control the relative value of N in shot-noise-unit (SNU) by adjusting the amplification parameter of homodyne detection (by controlling the power of LO or electronic amplifier). Usually, setting $N \in [3\sigma, 5\sigma]$ in SNU will attain performance close to the optimal strategy.

B. Effects of finite sampling resolution

The finite resolution n will make us lose the information about probability distribution of a inside discrete intervals $[(i-1/2)\Delta, (i+1/2)\Delta]$, $i \in \{-2^{n-1}, \dots, 2^{n-1}-1\}$ (as in Appendix A). Given a fixed N , the larger the n , the more information can be got about a . It is clear that the performance of the protocol will increase with resolution n as in Fig. 3. Given a fixed sampling range N , the effects of resolution n are:

1. If n is small (Δ is large), one cannot estimate precisely the CM of ρ_A (see Appendix C), thus overestimate the variance of quadratures for ρ_A and Eve's information $S(a_i : E)$. Furthermore, most measurement results lie in central bins (see Appendix A), which will reduce the Shannon entropy significantly (almost linearly) as in Fig. 3.
2. The classical information $H(a_i)$ increases almost linearly with n , while the estimated Eve's information reduces with n . As a result, the total extractable randomness will increase with n (as in Fig. 3).

In practice, given a fixed N , one should choose a larger n to attain better performance.

C. Effects of excess noise

In our protocol, the detection is assumed to be trusted and well characterized, and all the excess noise is due to a quantum correlated Eve. The excess noise or QCNR mainly decides the correlation between Eve's quantum state and Alice's

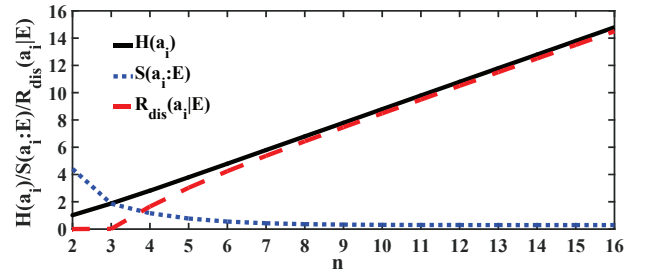


FIG. 3. (color online) Simulation results for Shannon entropy $H(a_i)$ of Alice's measurement results, upper bound of Eve's information $S(a_i : E)$ and extractable quantum randomness $R_{dis}(a_i|E)$ as a function of resolution n with sampling range $N = 5$. The simulations of $H(a_i)$ and $S(a_i : E)$ follows the same methods as in Fig. 2. The excess noise is chosen to be $\varepsilon = 0.1$ and ρ_A is assumed to be a symmetric Gaussian state with $V_x = V_p = 1 + \varepsilon$.

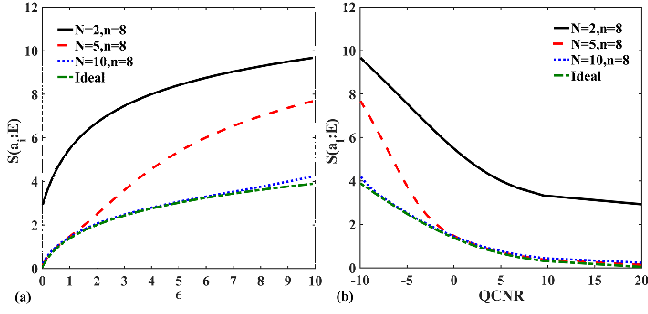


FIG. 4. (color online) Simulation results for upper bound of Eve's information $S(a_i : E)$ as a function of (a) excess noise and (b) QCNR, with $n = 8$ and $N = 2, 5, 10$, respectively. The ideal case corresponds to the estimated upper bound of $S(a_i : E)$ when $N \rightarrow \infty, n \rightarrow \infty$. ρ_A is assumed to be a symmetric Gaussian state with $V_x = V_p = 1 + \varepsilon$.

measurement results, which is a key parameter in security analysis. It is clear that $S(a_i : E)$ increases (decreases) with ε (QCNR), and one needs to choose proper N and n to get a tighter upper bound on $S(a_i : E)$. For a given n , the optimal value N varies with different QCNR, as in Fig. 4. For given N and ε , one can obtain a tighter bound of $S(a_i : E)$ with larger n , as in Fig. 5. Even when excess noise is much larger than quantum noise, one still can get a tight bound on Eve's information.

The final performance of the protocol is resistant against to the excess noise as shown in Fig. 6. More surprisingly, even if the QCNR goes below 0 (e.g. -10 dB), that is, excess noise due to Eve becomes larger than quantum noise, one can still obtain a nonzero number of certified random bits that are independent of Eve's side information. This means one can use high bandwidth commercial balanced receivers which does not require the receiver's high QCNR (e.g. ≥ 10 dB) as in former CV-QRNG experiment based on vacuum fluctuation [20–22] or CV-QKD experiment, and thus dramatically increases the random number generation rates.

An interesting and important question is what is the re-

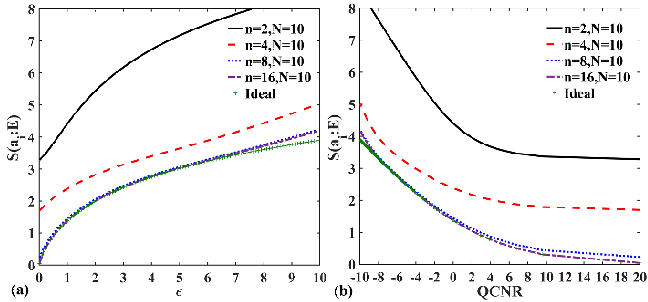


FIG. 5. (color online) Simulation results for upper bound of Eve's information $S(a_i : E)$ as a function of (a) excess noise and (b) QCNR, with $N = 10$ and $n = 2, 4, 8, 16$, respectively. The ideal case corresponds to the estimated value of $S(a_i : E)$ when $N \rightarrow \infty, n \rightarrow \infty$. ρ_A is assumed to be a symmetric Gaussian state with $V_x = V_p = 1 + \varepsilon$.

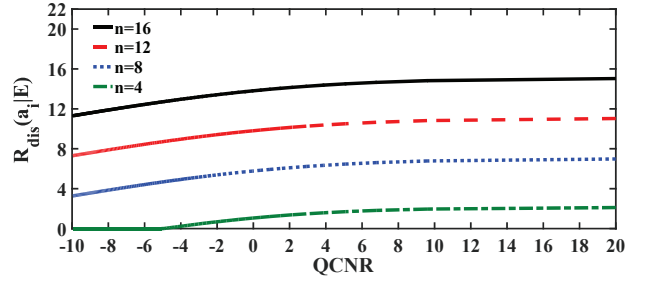


FIG. 6. (color online) Simulation results for extractable quantum randomness $R_{dis}(a_i|E)$ as a function of QCNR with $n = 4, 8, 12, 16$, respectively. The sampling range is chosen numerically optimally to be $N = 3.3\sigma$. ρ_A is assumed to be a symmetric Gaussian state with $V_x = V_p = 1 + \varepsilon$.

lationship between the system configuration and the maximal tolerable excess noise, or equivalently, the lowest QCNR that still keeps the extractable randomness non-negative. Intuitively, no matter how low the QCNR is, there is always some quantum randomness existing in the measurement results, which can be extracted as long as the resolution n is high enough, *i.e.*, at least to let the quantum randomness part change one bit of the measurement result. Considering that the Gaussian state extremality theorem and the assumption that Eve holds the purification of the whole state are used to estimate $R_{dis}(a_i|E)$, it is natural to ‘*imagine*’ the whole state is a two-mode squeezed state with variance σ^2 . In principle, Eve could provide X -squeezed states to Alice to gain more advantage than vacuum states, due to its reduced variance $V_x^{sq} = 1/\sigma^2$, since the final random bits are extracted only from the X -quadrature measurements. Thus, we predict that, if the quantum randomness are contained in two or more bins, *i.e.*, $[-\Delta_{max}, +\Delta_{max}] \in [-3\sqrt{V_x^{sq}}, +3\sqrt{V_x^{sq}}]$ ($\rightarrow \Delta_{max} \leq \frac{k}{\sigma}, k \approx 3$), then $R_{dis}(a_i|E)$ will be non-negative.

We check the prediction numerically with conditions $n = 8, 12, 16$ and different QCNRs. In Fig. 7 (a), $R_{dis}(a_i|E)$ with several typical QCNRs (-10 dB, -20 dB, -30 dB) are shown, and it is found $k \approx 3.05$, which is almost the same for other different QCNRs (see the black solid line in Fig. 7 (b)). However, if taking into consideration the modification of $\sqrt{V_x}$ as in Appendix C, it requires higher resolution n (smaller bin width Δ_{max} , see the red dashed line in Fig. 7 (b)).

V. EXPERIMENTAL IMPLEMENTATION AND PERFORMANCE

To validate the proposed protocol, a SI-CV-QRNG experimental setup is built based on balanced homodyne receiver to measure the vacuum fluctuations as in Fig. 8. We implemented an all-in-fiber setup with off-the-shelves devices. The local oscillator (LO) is a narrow line 1550 nm laser (Thorlabs SLF1550P, linewidth 50 KHz), and the LO power is carefully adjusted to obtain the optimal performance. The 50:50 beamsplitter (BS) brings LO signal interfered with the

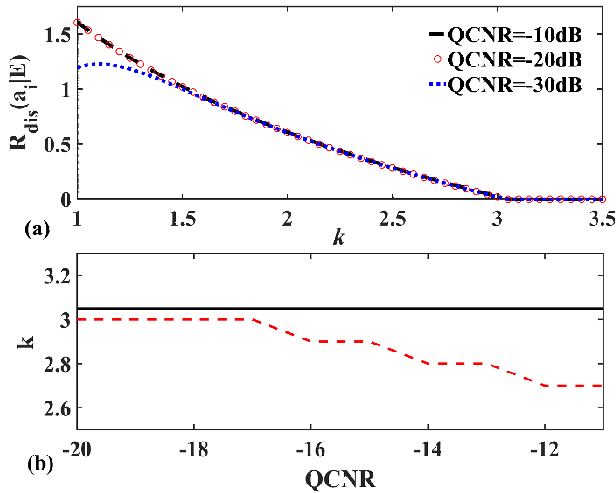


FIG. 7. (color online) (a) Simulation results for extractable quantum randomness $R_{dis}(a_i|E)$ as a function of $k = \Delta\sigma$ with $n = 16$ and QCNR = $-10dB$, $-20dB$, $-30dB$, respectively. Quiet similar results are found for $n = 8, 12$. In the simulations, we ignore the effects of digitization on estimation of CM to give an insight into the effect of parameter k . (b) The maximal allowed resolution $\Delta_{max} = k/\sigma$ for low QCNRs ($\leq -10dB$) with $n = 16$. Quiet similar results are found for $n = 8, 12$. The effects of digitization on estimation of CM are ignored in black solid line and considered in red dashed line.

vacuum states to the balanced receiver (Thorlabs PDB480C, bandwidth 1.6GHz). The phase of LO is randomly shifted between 0 and $\pi/2$ by a phase modulator (PM) to realized the random sampling between X and P quadratures measurements, based on an initial random seed t . Finally, the measurement results of the balanced receiver are sampled in real-time by a 12-bit ADC (TI ADC12D1800, bandwidth 3.5GHz) with a sampling rate of 1.8G SPS to acquire the raw data, which is to be analyzed by the proposed model to extract secure randomness.

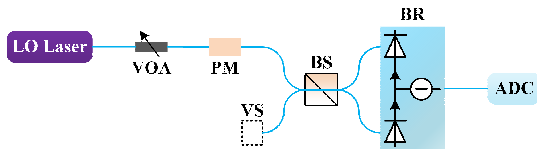


FIG. 8. (color online) Experimental setup of the proposed SI-CV-QRNG. LO: local oscillator, VOA: variable optical attenuator, PM: phase modular, BS: 50/50 beam splitter, VS: vacuum state, BR: balanced homodyne receiver, ADC: analog-to-digital converter. The CV-QRNG is realized with off-the-shelves components.

To obtain optimal performance, the LO power is increased from 0 mW with a fixed step of 0.5 mW and the voltage variance of the raw data corresponds to each LO power value is calculated and recorded, which is shown in Fig. 9. In the region from 0 mW to 9.5 mW, the variance of the sampled raw data enhances linearly with the increase of the LO power and the peak value is observed at the LO power value of 10 mW

due to the saturation of the balanced homodyne receiver. The LO power is fixed at 10 mW in the experiment to obtain optimal performance. The variance of the sampled raw data has a non-zero value even when the LO power is turned off, which is generally attributed to the classical noise resulted from the electromagnetic disturbance, the thermal fluctuations, the imperfection of the experimental setup and even the manipulation of eavesdroppers. In practical implementation, the classical noise can hardly be eliminated and will also be sampled into the raw data, resulting in an equivalently impure quantum states and impairing the randomness and security.

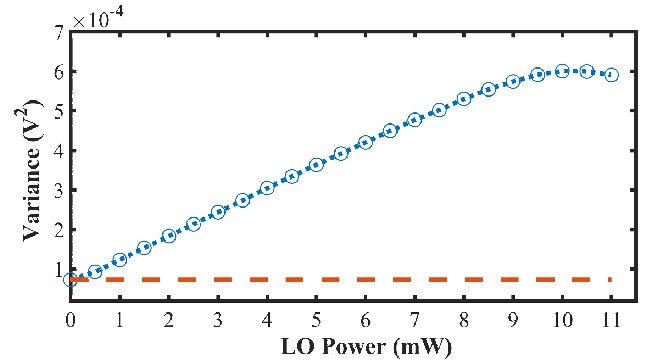


FIG. 9. (color online) Variance vs LO power. This figure shows the voltage variance of the sampled raw data as a function of the LO power. In the region from 0mW to 9.5 mW, it shows a relatively clear linearity between the voltage variance and the sampled raw data. While the LO power increases higher than 9.5 mW, the detection and amplification in the balanced receiver starts to saturate, resulting in the decrease of the linearity, and the peak value of the voltage variance is obtained at 10 mW.

To measure the vacuum fluctuations with respect to the excess noise, the measurements in the frequency domain have been performed by using an RF spectrum analyzer, which is shown in Fig. 10. Two different spectra have been acquired: the vacuum fluctuations when the LO power is 10 mW (red line) and the electrical noise when the LO power is turned off (blue line). From the figure we can see that in the detected range, the power of vacuum fluctuations is obviously higher than that of the electrical noise (the average gap between them is about 8.37dB within 0~1.6 GHz), which means the vacuum fluctuations dominate the output and demonstrates the effectiveness of the detection.

We present the results obtained on a typical run of $n_{tot} = 2.6214 \times 10^9$ data samples. The corresponding measured shot noise variance is $5.5572 \times 10^{-4} V^2$, excess noise variance is $6.31 \times 10^{-5} V^2$, and the total measurement results variance of X quadratures is $6.1182 \times 10^{-4} V^2$. In SNU, the variance of the pure vacuum state is normalized to 1, while the experimentally measured X quadrature variance is $\sigma^2 = 1.1135$ as shown in Fig. 11. As mentioned above, the deviation is mainly resulted from the classical noise in our experiment, which cannot be separated from the vacuum fluctuations in measurement results, leading to the impurity of the sampled raw data and the potential impairment of the

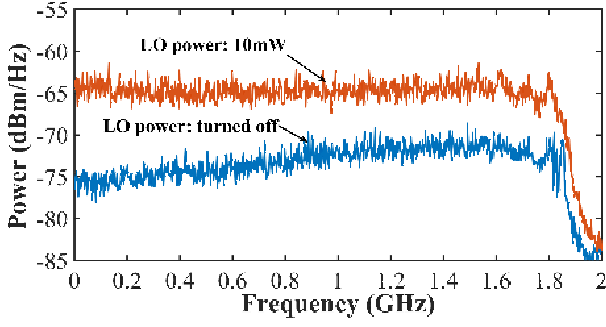


FIG. 10. (color online) The power spectral density of the vacuum fluctuations when the LO power is 10mW (red line) and the electrical noise when the LO power is turned off (blue line). Within the detected frequency range, the vacuum fluctuations dominate in terms of the power.

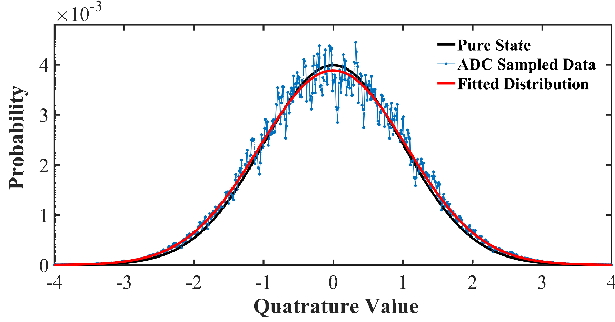


FIG. 11. (color online) The probability distribution of the ideal pure vacuum state (black line), the probability distribution of the ADC sampled raw data (blue line) in shot-noise-unite and the fitted distribution for raw data (red line).

security. The sampling range $N = 21.2098 = 20.0998\sigma$ and excess noise $\varepsilon = 0.1135$ in SNU, and the resolution $n = 12$. The estimated upper bound $\bar{V}_x = 1.1218$ and $\bar{V}_p = 1.1220$ in real experiment with the methods in Appendix C (the corresponding theoretical simulation results based on our model is $\bar{V}_x = \bar{V}_p = 1.1223$ for both quadratures under Gaussian assumption as in Eq. (11)). The experimental estimation and corresponding theoretical simulation of Shannon entropy, von Neumann entropy and extractable randomness are $H(a_i) = 8.7117(Exp)/8.7180(Theo)$, $S(\rho_A^G) = 0.3366(Exp)/0.3373(Theo)$ and $R_{dis}(a_i|E) = 8.3751(Exp)/8.3807(Theo)$, respectively. Furthermore, the number of bits necessary for the switching between the two quadratures must be accounted. Following [51], we set $n_c = \sqrt{n_{tot}}$. Out of the n_{tot} measurements, the check instants can be chosen in $\binom{n_{tot}}{n_c}$ different ways, which can be encoded in a seed $t = \lceil \log_2 \frac{n_{tot}!}{n_c!(n_{tot}-n_c)!} \rceil$ bits long. The final secure generation rate, i.e. true random bits per measurement, is

$$R_{sec} = \frac{1}{n_{tot}} [(n_{tot} - n_c)(H(a_i) - S(a_i : E)) - t]. \quad (12)$$

Given $n_{tot} = 2.6214 \times 10^9$, we employed $n_c = 5.12 \times 10^4$ bits to evaluate the extractable randomness, and $t = 8.7482 \times 10^5$. In our experiments, the corresponding secure rate of every measurement is $R_{sec} = 8.3746$ bits with sampling rate 1.8G SPS, which indicates an equivalent secure bit generation rate of 15.07 Gbits/s.

The final generated random bits sequences have passed all the NIST and DIEHARD tests.

VI. CONCLUSION AND DISCUSSION

We have proposed and experimentally demonstrated a SI-CV-QRNG protocol even if the source is untrusted or controlled by Eve. Based on the extremality of Gaussian states, a new theoretical model to estimate the lower bound on the extractable quantum randomness is established, which is similar to the security analysis of CV-QKD. The protocol is resistant to classical noise and losses (can be easily compensated by increasing LO power), which is beneficial for practical applications. The random numbers are sampled in real-time by a dedicated ADC hardware rather than oscilloscope [51], which is beneficial to a practical QRNG design. We experimentally demonstrate the protocol with commercial devices, and the final secure random number generation rate reaches up to 15 Gbits/s, which is much higher than previous SI-QRNG results [50, 51] and shows feasibility of the protocol with an ultra-fast, cheap and compact CV-QRNG. By using high bandwidth commercial balanced receivers and fast LO phase shifter, the secure generation rate can be increased to tens of Gbits/s.

The finite-size analysis should be investigated in further research, where one can use the fruitful theoretical tools built in CV-QKD. The SI-QRNG protocol proposed here is actually a CV-QKD protocol with a trivial sender, who always sends the vacuum state. Therefore, one can follow the same universal composable framework (UCF) in Ref. [57–60]. However, the finite-size analyze of SI-QRNG has two main differences with CV-QKD under UCF, i.e., no need for error correction, and only one parameter is statistically counted and tested in parameter estimation test. The core of finite-size analysis is to evaluate Eve's information about the measured random bit sequence, represented by a quantity of smooth min-entropy $H_{min}^{\varepsilon'}(a_i^{n_Q}|E)_{\rho^{n_Q}}$ that varies with data block size.

Further improvements can be envisaged when squeezed states are used as input state or heterodyne detection are used as measurement device for the protocol, which can be easily analyzed by the proposed security analysis methods. In this paper, the LO power is assumed to be constant and fixed. Furthermore, security analysis against the LO power fluctuation needs to be further investigated. In our lab experiment, the LO power is relatively stable. However, in practical application, it could be influenced by the environment or even by Eve.

This work is supported by National Natural Science Foundation of China (Grant No. 61771439, 61501414, 61702469, 61602045), National Cryptography Development Fund (Grant No. MMJJ20170120), Sichuan Youth Science and Technology Foundation(Grant No. 2017JQ0045), Foundation of Sci-

ence and Technology on Communication Security Laboratory (Grant No. 6142103040105).

Appendix A: Model of coarse-grained homodyne measurement

We model Alice's real-life coarse-grained homodyne measurement process into two steps. Firstly, Alice uses an ideal homodyne detector to measure the quadrature of input states with continuous output a following probability distribution $p(a)$, which cannot be read. Secondly, Alice digitizes the continuous variable a into n digitized bits a_i following probability distribution $p_{dis}(a_i)$ by an ADC with sampling range N and resolution n [23, 51], which is the actual output of a real-life homodyne detector. To be precise, Alice digitizes the data a between $[-N + \Delta/2, N - \Delta/2]$ into 2^n equal intervals with bin width $\Delta = N/2^{n-1}$. The range is chosen so that the central bin is centered at zero. The central value of each interval represents the digitized results, while for data smaller than $-N$ or greater than N it will be the smallest and the largest digitized value. Then, one has,

$$a_i = \begin{cases} a_{-2^{n-1}} \equiv -N & a < -N + \Delta/2 \\ a_{-2^{n-1}+1} \equiv -N + \Delta & -N + \Delta/2 \leq a < -N + 3\Delta/2 \\ a_{-2^{n-1}+2} \equiv -N + 2\Delta & -N + 3\Delta/2 \leq a < -N + 5\Delta/2 \\ \vdots & \vdots \\ a_0 \equiv 0 & -\Delta/2 \leq a < \Delta/2 \\ a_1 \equiv \Delta & \Delta/2 \leq a < 3\Delta/2 \\ \vdots & \vdots \\ a_{2^{n-1}-3} \equiv N - 3\Delta & N - 7\Delta/2 \leq a < N - 5\Delta/2 \\ a_{2^{n-1}-2} \equiv N - 2\Delta & N - 5\Delta/2 \leq a < N - 3\Delta/2 \\ a_{2^{n-1}-1} \equiv N - \Delta & a \geq N - 3\Delta/2 \end{cases}, \quad (\text{A1})$$

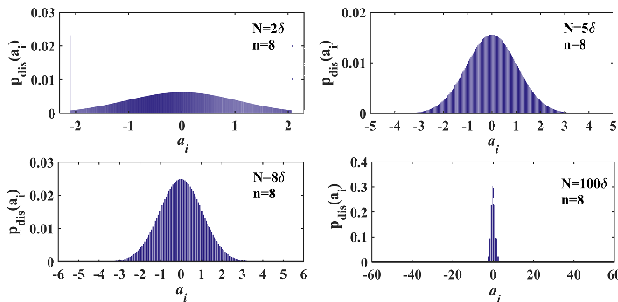


FIG. 12. (color online) Simulation results of the probability distribution $p_{dis}(a_i)$ of Alice's measurement results a_i with different sampling range $N = 2\sigma, 5\sigma, 8\sigma$ and 100σ by Eq. (A4) under Gaussian assumption. The resolution is fixed to be $n = 8$ and the excess noise is chosen to be $\varepsilon = 0.1$.

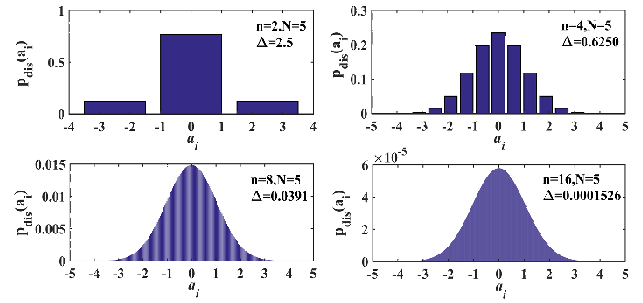


FIG. 13. (color online) Simulation results of the probability distribution $p_{dis}(a_i)$ of Alice's measurement results a_i with different resolution $n = 2, 4, 8$ and 16 by Eq. (A4) under Gaussian assumption. The sampling range is fixed to be $N = 5$ and the excess noise is chosen to be $\varepsilon = 0.1$.

where $i \in \{-2^{n-1}, \dots, 2^{n-1} - 1\}$. The probability distribution $p_{dis}(a_i)$ reads,

$$p_{dis}(a_i) = \begin{cases} \int_{-N+\Delta/2}^{-\infty} p(a) da & i = i_{\min} \\ \int_{a_i+\Delta/2}^{a_i-\Delta/2} p(a) da & i_{\min} < i < i_{\max} \\ \int_{+\infty}^{N-3\Delta/2} p(a) da & i = i_{\max} \end{cases} \quad (\text{A2})$$

Suppose a follows Gaussian distribution with variance $\sigma^2 = 1 + \varepsilon$ and null mean value,

$$p(a) = \frac{1}{\sqrt{2\pi\sigma}} \exp\left(-\frac{a^2}{2\sigma^2}\right), \quad (\text{A3})$$

which is a typical result in vacuum fluctuation measurement. Then,

$$p_{dis}^G(a_i) = \begin{cases} \frac{1}{2} \operatorname{erfc}\left(\frac{N-0.5\Delta}{\sqrt{2}\sigma}\right), & i = i_{\min} \\ \frac{1}{2} \operatorname{erf}\left(\frac{i+0.5\Delta}{\sqrt{2}\sigma}\right) - \frac{1}{2} \operatorname{erf}\left(\frac{i-0.5\Delta}{\sqrt{2}\sigma}\right), & i_{\min} < i < i_{\max} \\ \frac{1}{2} \operatorname{erfc}\left(\frac{N-1.5\Delta}{\sqrt{2}\sigma}\right), & i = i_{\max} \end{cases} \quad (\text{A4})$$

Simulation results of the probability distribution $p_{dis}(a_i)$ with different sampling range and fixed resolution are shown in Fig. 12. It is shown that a_i becomes more predictable when N is too small (or large) due to the oversaturated (or unoccupied) measurement results, which will reduce the extractable randomness.

Simulation results of the probability distribution $p_{dis}(a_i)$ with different resolution and fixed sampling range are shown in Fig. 13. If it is small, most measurement results lie in central bins, which will reduce the Shannon entropy dramatically. The larger the resolution, the better the extractable randomness.

Appendix B: $S(a_i : E) \leq S(a : E)$

Suppose Alice's measurement results of an ideal and a coarse-grained homodyne measurement on X quadratures of

quantum state ρ_A are a and a_i (as in Appendix A), respectively, and denote the corresponding quantum state hold by Eve is $\rho_{E|a}$ and $\rho_{E|a_i}$, respectively. Then one has

$$\rho_E = \int p(a) \rho_{E|a} da, \quad (\text{B1})$$

and

$$\rho_{E|a_i} = \begin{cases} \int_{-\infty}^{-N+\frac{1}{2}\Delta} \frac{p(a)}{p_{dis}(a_i)} \rho_{E|a} da & i = i_{\min} \\ \int_{a_i-\frac{1}{2}\Delta}^{a_i+\frac{1}{2}\Delta} \frac{p(a)}{p_{dis}(a_i)} \rho_{E|a} da & i_{\min} < i < i_{\max} \\ \int_{N-\frac{3}{2}\Delta}^{+\infty} \frac{p(a)}{p_{dis}(a_i)} \rho_{E|a} da & i = i_{\max} \end{cases} \quad (\text{B2})$$

Note that $p(a)$ is unknown to Alice. Thus, the total system is assumed to be

$$\rho_{AE}^{dis} = \sum_{i=i_{\min}}^{i=i_{\max}} p_{dis}(a_i) |a_i\rangle \langle a_i| \otimes \rho_{E|a_i} \quad (\text{B3})$$

One can easily verify that the overall state of Eve is the same as the ideal case,

$$\rho_E^{dis} = \text{tr}(\rho_{AE}^{dis}) = \text{tr}(\rho_{AE}) = \rho_E. \quad (\text{B4})$$

Using Holevo's bound, one has

$$I(a_i : E) \leq S(a_i : E) = S(\rho_E^{dis}) - \sum_{i=i_{\min}}^{i=i_{\max}} p_{dis}(a_i) S(\rho_{E|a_i}). \quad (\text{B5})$$

Using the concavity of the von Neumann entropy,

$$S(\rho_{E|a_i}) = S\left(\int_{a_i-\frac{1}{2}\Delta}^{a_i+\frac{1}{2}\Delta} \frac{p(a)}{p_{dis}(a_i)} \rho_{E|a} da\right) \geq \int_{a_i-\frac{1}{2}\Delta}^{a_i+\frac{1}{2}\Delta} \frac{p(a)}{p_{dis}(a_i)} S(\rho_{E|a}) da, \quad (\text{B6})$$

(similar for $i = i_{\min}$ and i_{\max}). Then, one can get

$$\begin{aligned} I(a_i : E) &\leq S(a_i : E) = S(\rho_E^{dis}) - \sum_{i=i_{\min}}^{i=i_{\max}} p_{dis}(a_i) S(\rho_{E|a_i}) \\ &\leq S(\rho_E) - \int_{-\infty}^{+\infty} p(a) S(\rho_{E|a}) da = S(E : a) \end{aligned} \quad (\text{B7})$$

Qualitatively speaking, the digitization process can have a corresponding quantum operation acting only on Alice's side, while the operation conducting only on one part of the state can not increase the mutual information between two parties.

Appendix C: Effects of digitization on estimation of CM

The upper bound of $S(\rho_A)$ for ρ_A can be calculated by considering it is a Gaussian state with the same CM using Gaussian extremality theorem. The real CM for ρ_A should be estimated through Alice's ideal detection result a , which is continuous, noted by

$$\gamma_A = \begin{pmatrix} V_x & c \\ c & V_p \end{pmatrix}, \quad (\text{C1})$$

with symplectic eigenvalue $\lambda = \sqrt{\det(\gamma_A)} = \sqrt{V_x V_p - c^2}$, where V_x , V_p and c are real numbers. The von Neumann entropy of a Gaussian state with CM γ_A is

$$S(\rho_A^G) = \frac{\lambda+1}{2} \log_2 \frac{\lambda+1}{2} - \frac{\lambda-1}{2} \log_2 \frac{\lambda-1}{2} \geq S(\rho_A). \quad (\text{C2})$$

To estimate the upper bound of $S(\rho_A^G)$, one only needs to upper bound the symplectic eigenvalue, which is equivalent to upper bound V_x and V_p , lower bound c^2 .

In ideal digitization with infinite sampling range, the upper bound of $V_x(V_p)$ is easy to get, since each unknown a is upper and lower bounded by its digitization interval, *i.e.*, $a_i - \frac{1}{2}\Delta \leq a \leq a_i + \frac{1}{2}\Delta$. Therefore, for $a_i \leq 0$ we use $a_i - \frac{1}{2}\Delta$, and for $a_i > 0$ we use $a_i + \frac{1}{2}\Delta$ to calculate V_x , which is an upper bound. However, in a real system, the digitization has finite sampling range. For asymptotic case, an extra energy test is needed for the most rigorous proof. For a approximate but more practical solution, we can set a relatively large bound $[-a_{\lim}, a_{\lim}]$, in which the probability of the case $a \notin [-a_{\lim}, a_{\lim}]$ is negligible. For example, for a Gaussian distributed a with variance σ^2 , if $a_{\lim} = 10\sigma$, then $Pr[a \notin [-a_{\lim}, a_{\lim}]] < 1.5 \times 10^{-23}$; and if $a_{\lim} = 100\sigma$, then $Pr[a \notin [-a_{\lim}, a_{\lim}]] < 5.5 \times 10^{-89}$. The V_x is upper bounded by the following quantity with high confidence level,

$$\begin{aligned} \bar{V}_x &= p_{dis}(a_{i_{\min}}) a_{i_{\min}}^2 + p_{dis}(a_{i_{\max}}) a_{i_{\max}}^2 \\ &+ \sum_{i=i_{\min}+1}^0 p_{dis}(a_i) \left(a_i - \frac{1}{2}\Delta\right)^2 + \sum_{i=1}^{i_{\max}-1} p_{dis}(a_i) \left(a_i + \frac{1}{2}\Delta\right)^2. \end{aligned} \quad (\text{C3})$$

Similarly, one can upper bound the variance of P quadrature with the same methods, $\bar{V}_p \geq V_p$. For simplicity, we set $c = 0$ to upper bound Eve's information. Finally, the upper bound of the symplectic eigenvalue for ρ_A is $\bar{\lambda} = \sqrt{\bar{V}_x \bar{V}_p}$, and

$$S(\rho_A) \leq \frac{\bar{\lambda}+1}{2} \log_2 \frac{\bar{\lambda}+1}{2} - \frac{\bar{\lambda}-1}{2} \log_2 \frac{\bar{\lambda}-1}{2}. \quad (\text{C4})$$

The effects of sampling range N and resolution n on estimated upper bound of quadrature variance is shown in Fig. 14

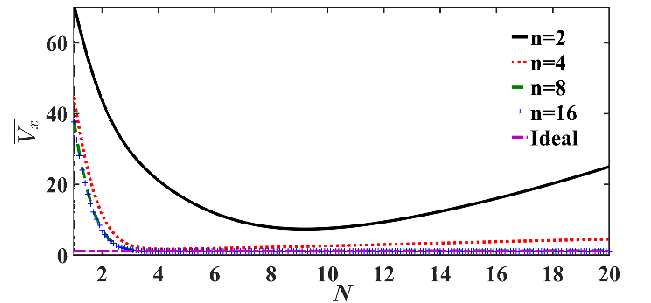


FIG. 14. (color online) The simulation results for upper bound of quadratures variance \bar{V}_x (\bar{V}_p) for ρ_A based on Alice's digitized measurement results as a function of sampling range N with resolution $n = 2, 4, 8, 16$, respectively. The ideal case corresponds to the estimated value of V_x when $N \rightarrow \infty, n \rightarrow \infty$. The excess noise is chosen to be $\varepsilon = 0.1$.

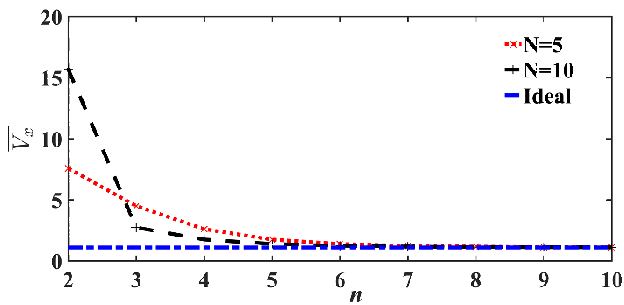


FIG. 15. (color online) The simulation results for upper bound of quadratures variance \bar{V}_x for ρ_A based on Alice's digitized measurement results as a function of resolution n and range $N = 5, 10$, respectively. The ideal case corresponds to the estimated value of V_x when $N \rightarrow \infty, n \rightarrow \infty$. The excess noise is chosen to be $\varepsilon = 0.1$.

and Fig. 15, respectively. Generally, one can get a tighter upper bound \bar{V}_x by increasing n . When $N < 3\sigma$, one will overestimate the variance of a based on measurement results a_i , which will significantly overestimate Eve's information.

For the finite-size case, we can choose a relatively large sampling range N , and set the bound of energy test within $[-N, N]$. And we further require that even if only one digitized data exceeds the energy test bound, the energy test for the whole block fails. Therefore, for all the data blocks that pass the energy test, the upper bound of the estimated V_x can be got through the same strategy as above. For the data blocks fail the energy test, this round of the protocol aborts. One should note that, the sampling range should be carefully chosen, if it's too small, too many blocks will fail; if it's too large, the estimated parameter will be too pessimistic.

-
- [1] B. Hayes, *Randomness as a resource*, American Scientist **89**, 300 (2001).
- [2] V. Scarani, H. Bechmannpasquinucci, N. J. Cerf, M. Düsek, N. Lütkenhaus, and M. Peev, *The security of practical quantum key distribution*, Rev. Mod. Phys. **81**, 1301 (2008).
- [3] N. Gisin, G. Ribordy, W. Tittel, and H. Zbinden, *Quantum cryptography*, Rev. Mod. Phys. **74**, 145 (2002).
- [4] J. Bouda, M. Pivoluska, M. Plesch, and C. Wilmott, *Weak randomness seriously limits the security of quantum key distribution*, Phys. Rev. A **86**, 062308 (2012).
- [5] P. Li, Y. Sun, X. Liu, X. Yi, J. Zhang, X. Guo, Y. Guo, and Y. Wang, *Fully photonics-based physical random bit generator*, Opt. Lett. **41**, 3347 (2016).
- [6] M. N. Bera, A. Acin, M. Kus, M. Mitchell, and M. Lewenstein, *Randomness in Quantum Mechanics: Philosophy, Physics and Technology*, arXiv: 1611.02176 (2016).
- [7] X. Ma, X. Yuan, Z. Cao, B. Qi, and Z. Zhang, *Quantum random number generation*, npj Quantum Information **2**, 16021 (2016).
- [8] M. Herrero-Collantes and J. C. Garcia-Escartin, *Quantum Random Number Generators*, Rev. Mod. Phys. **89**, 015004 (2017).
- [9] T. Jennewein et al. *A fast and compact quantum random number generator*, Rev. Sci. Instrum. **71**, 1675 (2000).
- [10] A. Stefanov et al. *Optical quantum random number generator*, J. Mod. Opt. **47**, 595 (2000).
- [11] J. F. Dynes, et al. *A high speed, postprocessing free, quantum random number generator*, Appl. Phys. Lett. **93**, 031109 (2008).
- [12] M. Wayne, et al. *Photon arrival time quantum random number generation*, J. Mod. Opt. **56**, 516 (2009).
- [13] M. Wahl, et al. *An ultrafast quantum random number generator with provably bounded output bias based on photon arrival time measurements*, Appl. Phys. Lett. **98**, 171105 (2011).
- [14] Y. Q. Nie, et al. *Practical and fast quantum random number generation based on photon arrival time relative to external reference*, Appl. Phys. Lett. **104**, 051110 (2014).
- [15] H. Q. Ma, et al. *Random number generation based on the time of arrival of single photons*, Appl. Opt. **44**, 7760 (2005).
- [16] H. Furst, et al. *High speed optical quantum random number generation*, Opt. Express **18**, 13029 (2010).
- [17] M. Ren, et al. *Quantum random-number generator based on a photon-number-resolving detector*, Phys. Rev. A **83**, 023820 (2011).
- [18] M. Applegate, et al. *Efficient and robust quantum random number generation by photon number detection* Appl. Phys. Lett. **107**, 071106 (2015).
- [19] W. Wei and H. Guo, *Bias-free true random-number generator*, Opt. Lett. **34**, 1876 (2009).
- [20] C. Gabriel, C. Wittmann, D. Sych, R. F. Dong, W. Maurer, U. L. Andersen, C. Marquardt, and G. Leuchs, *A generator for unique quantum random numbers based on vacuum states*, Nature Photonics **4**, 711 (2010).
- [21] Y. Shen, L. A. Tian, and H. X. Zou, *Practical quantum random number generator based on measuring the shot noise of vacuum states*, Phys. Rev. A **81**, 063814 (2010).
- [22] T. Symul, S. M. Assad, and P. K. Lam, *Real time demonstration of high bitrate quantum random number generation with coherent laser light*, Appl. Phys. Lett. **98**, 231103 (2011).
- [23] J. Y. Haw, S. M. Assad, A. M. Lance, N. H. Y. Ng, V. Sharma, P. K. Lam, and T. Symul, *Maximization of Extractable Randomness in a Quantum Random Number Generator*, Phys. Rev. Applied **3**, 054004 (2015).
- [24] F. Raffaelli, G. Ferrantiz, D. H. Mahler, P. Sibson, J. E. Kennard, A. Santamato, G. Sinclair, D. Bonneau, M. G. Thompson, and J. C. F. Matthews, *An On-chip Homodyne Detector for Measuring Quantum States and Generating Random Numbers*, arXiv: 1612.04676 (2016).
- [25] Q. Zhou, R. Valivarthi, C. John, and W. Tittel, *Practical quantum random number generator based on sampling vacuum fluctuations*, arXiv:1703.00559 (2017).
- [26] B. Qi, Y. M. Chi, H. K. Lo, and L. Qian, *High-speed quantum random number generation by measuring phase noise of a single-mode laser*, Opt. Lett. **35**, 312 (2010).
- [27] H. Guo, W. Z. Tang, Y. Liu, and W. Wei, *Truly random number generation based on measurement of phase noise of a laser*, Phys. Rev. E **81**, 051137 (2010).
- [28] M. Jofre, et al. *True random numbers from amplified quantum vacuum*, Opt. Express **19**, 20665 (2011).
- [29] F. Xu, et al. *Ultrafast quantum random number generation based on quantum phase fluctuations*, Opt. Express **20**, 12366 (2012).
- [30] Z. Yuan, et al. *Robust random number generation using steady-state emission of gain-switched laser diodes*, Appl. Phys. Lett.

- 104**, 261112 (2014).
- [31] C. Abellan, et al. *Ultra-fast quantum randomness generation by accelerated phase diffusion in a pulsed laser diode*, *Opt. Express* **22**, 1645 (2014).
- [32] Y. Q. Nie, et al. *The generation of 68 Gbps quantum random number by measuring laser phase fluctuations*, *Rev. Sci. Instrum.* **86**, 063105 (2015).
- [33] X. G. Zhang, Y. Q. Nie, H. Y. Zhou, H. Liang, X. Ma, J. Zhang, and J. Pan, *Fully integrated 3.2 Gbps quantum random number generator with real-time*, *Rev. Sci. Instrum.* **87**, 076102 (2016).
- [34] J. Liu, J. Yang, Q. Su, Z. Li, F. Fan, B. J. Xu, and H. Guo, *117 Gbits/s quantum random number generation with simple structure*, *IEEE Photonics Technology Letters* **29**, 1109 (2017).
- [35] J. Yang, J. Liu, Q. Su, Z. Li, F. Fan, B. J. Xu, and H. Guo, *A 5.4 Gbps real time quantum random number generator with compact implementation*, *Opt. Express* **24**, 027474 (2016).
- [36] H. Zhou, et al. *Randomness generation based on spontaneous emissions of lasers*, *Phys. Rev. A* **91**, 062316 (2015).
- [37] C. R. S. Williams, J. C. Salevan, X. W. Li, R. Roy, and T. E. Murphy, *Fast physical random number generator using amplified spontaneous emission*, *Opt. Express* **18**, 23584 (2010).
- [38] X. W. Li, A. B. Cohen, T. E. Murphy, and R. Roy, *Scalable parallel physical random number generator based on a super-luminescent LED*, *Opt. Lett.* **36**, 1020 (2011).
- [39] A. Martin, B. Sanguinetti, C. C. W. Lim, R. Houlmann, and H. Zbinden, *Quantum random number generation for 1.25-GHz quantum key distribution systems*, *J. Lightwave Technol.* **33**, 2855 (2015).
- [40] W. Wei, G. Xie, A. Dang, and H. Guo, *High-speed and bias-free optical random number generator*, *IEEE Photonics Technology Letters* **24**, 437 (2012).
- [41] Y. Liu, M. Y. Zhu, B. Luo, J. W. Zhang, and H. Guo, *Implementation of 1.6 Tbs^{-1} truly random number generation based on a super-luminescent emitting diode*, *Laser Phys. Lett.* **10**, 045001 (2013).
- [42] J. Bell, *On the einstein-podolsky-rosen paradox*, *Physics* **1**, 195 (1964).
- [43] R. Colbeck, et al. *Private randomness expansion with untrusted devices*, *J. Phys. A* **4**, 095305 (2011).
- [44] S. Fehr, et al. *Security and composability of randomness expansion from bell inequalities*, *Phys. Rev. A* **87**, 012335 (2013).
- [45] C. A. Miller and Y. Shi, *Robust protocols for securely expanding randomness and distributing keys using untrusted quantum devices*, In *Proceedings of the 46th Annual ACM Symposium on Theory of Computing*, STOC'14, 417C426 (ACM, New York, NY, USA, 2014).
- [46] C. A. Miller and Y. Shi, *Universal security for randomness expansion*, arXiv:1411.6608 (2014).
- [47] S. Pironio, et al. *Random numbers certified by Bells theorem*, *Nature* **464**, 1021 (2010).
- [48] R. Colbeck and R. Renner, *Free randomness can be amplified*, *Nature Physics* **8**, 450 (2012).
- [49] R. Gallego, et al. *Full randomness from arbitrarily deterministic events*, *Nature Communications* **4**, 2654 (2013).
- [50] Z. Cao, et al. *Source-independent quantum random number generation*, *Phys. Rev. X* **6**, 011020 (2016).
- [51] D. G. Marangon, G. Vallone, and P. Villoresi, *Source-device-independent Ultra-fast Quantum Random Number Generation*, *Phys. Rev. Lett.* **118**, 060503 (2017).
- [52] J. B. Brask, A. Martin, W. Esposito, R. Houlmann, J. Bowles, H. Zbinden, and N. Brunner, *High-rate semi-device-independent quantum random number generators based on unambiguous state discrimination*, *Phys. Rev. Applied* **7**, 054018 (2017).
- [53] Z. Cao, H. Zhou, and X. Ma, *Loss-tolerant measurement-device-independent quantum random number generation*, *New J. Phys.* **17**, 125011 (2015).
- [54] Y. Q. Nie, J. Y. Guan, H. Y. Zhou, Q. Zhang, X. Ma, J. Zhang, and J. W. Pan, *Experimental measurement-device-independent quantum random number generation*, *Phys. Rev. A* **94**, 060301 (2016).
- [55] M. E. Wolf, G. Giedke, and J. I. Cirac, *Extremality of Gaussian Quantum States*, *Phys. Rev. Lett.* **96**, 080502 (2006).
- [56] R. Garcia-Patron and N. J. Cerf, *Unconditional optimality of Gaussian Attacks against continuous-variable quantum key distribution*, *Phys. Rev. Lett.* **97**, 190503 (2006).
- [57] A. Leverrier, *Composable Security Proof for Continuous-Variable Quantum Key Distribution with Coherent States*, *Phys. Rev. Lett.* **114**, 070501 (2015).
- [58] A. Leverrier, *Security of continuous-variable quantum key distribution via a Gaussian de Finetti reduction*, *Phys. Rev. Lett.* **118**, 200501 (2017).
- [59] C. Lupo, C. Ottaviani, P. Papanastasiou, and S. Pirandola, *Composable Security of Measurement-Device-Independent Continuous-Variable Quantum Key Distribution against Coherent Attacks*, arXiv: 1704.07924 (2017).
- [60] F. Furrer, T. Franz, M. Berta, A. Leverrier, V. B. Scholz, M. Tomamichel, and R. F. Werner, *Continuous Variable Quantum Key Distribution: Finite-Key Analysis of Composable Security against Coherent Attacks*, *Phys. Rev. Lett.* **109**, 100502 (2012).